Microscopic dynamics of highly permeable super glassy polynorbornenes revealed by quasielastic neutron scattering

Andreas Schönhals[1,*], Paulina Szymoniak[1], Mohamed A. Kolmangadi[1], Martin Böhning[1], Michaela Zamponi[2], Bernhard Frick[3], Markus Appel[3], Gerrit Günther[4], Margarita Russina[4], Dmitry A. Alentiev[5], Maxim Bermeshev[5], and Reiner Zorn[6]

[1]Bundesanstalt für Materialforschung und -prüfung (BAM), Unter den Eichen 87,12205 Berlin, Germany
[2]Forschungszentrum Jülich GmbH, Jülich Centre for Neutron Science at MLZ, Lichtenbergstr. 1, 85748 Garching, Germany
[3]Institut Laue Langevin, 71, Avenue des Martyrs, Grenoble 38000, France
[4]Helmholtz Zentrum Berlin, Hahn-Meitner Platz 1, 14109 Berlin, Germany
[5]A.V. Topchiev Institute of Petrochemical Synthesis of Russian Academy of Science, Leninskii prospect, 29, 119991 Moscow, Russia
[6]Forschungszentrum Jülich GmbH, Jülich Centre for Neutron Science (JCNS-1) and Institute for Biological Information Processing (IBI-8), 52425 Jülich, Germany

Abstract:

The molecular dynamics of addition-type poly(tricyclononenes) with Si-substituted bulky side groups has been investigated by a combination of neutron time-of-flight and neutron backscattering spectroscopy methods on a time scale from 0.1 ps to ca. 3 ns. The investigated poly(tricyclononenes) PTCNSi1 and PTCNSi2g both bear a high microporosity which makes them promising candidates for active separation layers for gas separation membranes. Pathways in the structure of the temporary network of micropores can be opened and closed for the diffusion of gas molecules. A low temperature relaxation process was found for both polymers by the performed neutron scattering experiments. This process was assigned to the methyl group rotation. It was analysed in terms of a jump diffusion in a three-fold potential. The analysis of the dependence of the elastic incoherent structure factor on the scattering vector yields the number of methyl groups which might be immobilized. For PTCNSi1 (3 methyl groups in the monomeric unit) it was found that all methyl groups take part in the methyl group rotation whereas for PTCNSi2g (6 methyl groups in monomeric unit) a considerable number of methyl groups are blocked in their rotation. This immobilization of methyl groups is due to the sterically demanding arrangement of the methyl groups in PTCNSi2g. This conclusion is further supported by the result that the activation energy for the methyl group rotation is three times higher for PTCNSi2g than that of PTCNSi1.

1. **INTRODUCTION**

Membrane processes, for instance for the separation of gases, are among the key technologies in sustainable energy supply. Compared to techniques based on absorption or cryogenic processes they are cost and energy efficient. Glassy polymers are belonging to the most interesting class of materials for the active separation layers in these membranes. Moreover, polymers can be processed at larger scales and are inexpensive in comparison to other materials.

The most attractive candidates for polymers in gas separation membranes are glassy polymers with a high free volume. The demand to optimize the polymeric materials stimulated an intensive development in the field and led for instance to the synthesis of polymers such as poly(trimethylsilylpropyne) (PTMSP)[1] and poly(4-methyl-2-pentyne) (PMP)[2,3]. For these polyacetylenes the level of permeability was found orders of magnitude higher than that of classical or conventional glassy polymers. The research also lead to the development of new classes of polymers with an extraordinary high free volume like polymers of intrinsic microporosity (PIMs)[4,5] or addition-type poly(norbornenes) or poly(tricyclononenes) [6-10] with Si-substituted bulky side groups. The microporosity of PIMs results from a rigid backbone having also spiro-centers which cause a contorted chain structure leading to an insufficient packing in the condensed state. In difference for the mentioned polynorbornenes in addition to stiff backbones the microporosity is mainly due to the bulky substituents. These substituents prevent also an effective packing of the segments in the condensed state. The microporosity is characterized by large values of Brunauer/Emmett/Teller (BET) surface areas of several hundred m^2/g. This goes along with a high free volume in the form of a continuous void phase.[11,12] The considered Si-substituted polynorbornenes/poly(tricyclononenes) exhibit, like PIMs, a favourable combination of reasonable permselectivities with high permeabilities values.[9,10]

Recently broadband dielectric spectroscopy was employed to investigate the molecular mobility of two Si-substituted polynorbornenes poly(3-(trimethylsilyl) tricyclononene-7) (PTCNSi1) and poly(3,3-bis(trimethylsilyl) tricyclononene-7) (PTCNSi2g).[13,14] Two relaxation processes were found for both polymers. The one found at lower temperatures or higher frequencies was assigned to localized fluctuations, whereas the process which was observed at higher temperatures corresponding to lower frequencies is related to Maxwell/Wagner/Sillars polarization effects induced by the microporosity of the polynorbornenes. Moreover, it should be noted that no glass transition temperature T_g could be estimated for the polynorbornenes/poly(tricyclononenes) prior to their thermal degradation by

conventional DSC. Molecular dynamic simulations gave some evidence that the T_g has to be expected close to the chemical decomposition temperature.[15]

The gas transport through dense polymer membranes is generally discussed in the framework of a solution diffusion model. While the solubility of a gas molecule depends mainly on its polarizability, the diffusivity depends on its effective size. For instance, this size can be characterized by the minimal diameter of a molecule allowing its transport through a rigid or dynamic bottleneck of the polymer matrix. In that respect the molecular mobility of the polymer must be considered. It can be discussed that due to molecular fluctuations, for instance the rotation of methyl groups, the connection between the free volume elements can be opened or closed. Quasielastic neutron scattering has been employed to investigate the molecular mobility of high-performance polymers.[16-18] Molecular fluctuations at a time scale of picoseconds are found to be relevant for the gas transport in polymers. Furthermore, the neutron data and the diffusion coefficient of gas molecules have been correlated.[16] Recently, also quasielastic neutron scattering has been utilized to investigate the molecular mobility of a polymer of intrinsic microporosity, PIM-1, in comparison to a conventional high-performance polyimide.[19]

Also the low frequency density of states was investigated for PTCNSi1 and PTCNSi2g by inelastic neutron scattering in a recent paper.[20]

2. EXPERIMENTAL SECTION

Materials.

Addition-type polymerization was employed to prepare the polymers investigated here.[7,8,] The chemical structures of PTCNSi1 and PTCNSi2g are depicted in Figure 1 together with an optimized model of their repeat units. PTCNSi1 has one trimethylsilyl side group while PTCNSi2g bears two. Therefore, the influence of the number of trimethylsilyl side groups could be discussed for these two polymers.

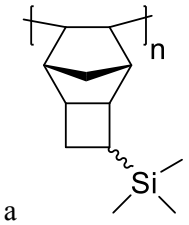

a

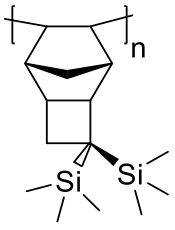

b

Figure 1: Chemical structure of the investigated polynorbornenes: a - PTCNSi1 and b – PTCNSi2g.

The molecular weights M_w were estimated by size exclusion chromatography to 550000 g/mol (PTCNSi1) and 350000 g/mol (PTCNSi2g) leading to good film forming properties. Both polymers have a distinct microporosity characterized by BET surface area values of 790 m^2/g (PTCNSi2g)[7] and 610 m^2/g (PTCNSi1).[7] As stated above, due to the rigid chain structure no glass transition temperature could be estimated for both polymers before their degradation.

For the details of the sample preparation the reader is referred to ref. [13,14]. In brief, solutions of both polymers in toluene were prepared with concentrations adapted to end up with a film thickness allowing for ca. 10 % incoherent neutron scattering. Such a film thickness minimizes effects due to multiple scattering. A 0.2 µm PVDF-filter was used to cast the solution into a Teflon mold. To control the evaporation of the solvent from the film, the mold was placed in a closed chamber with a saturated toluene atmosphere at room temperature. A solid film was obtained after ca. 3 days. To remove the solvent completely, the film was subsequently annealed in an oil-free vacuum at a temperature of 393 K (120 °C) for 3 days. The samples were then sealed hermetically in flat aluminum cells for the neutron scattering experiments because aluminum is nearly transparent for neutrons.

Neutron Scattering.

During a quasielastic neutron scattering experiment both, momentum and energy, are exchanged between the nuclei of the sample and the neutrons. Therefore, neutron scattering is sensitive to molecular motions at microscopic length scales and times.[22] The double differential cross section $\frac{d^2\sigma}{d\Omega\, d\omega}$ is the main experimental quantity obtained from a quasielastic neutron scattering experiment. It is given by

$$\frac{d^2\sigma}{d\Omega\, d\omega} = \frac{1}{4\pi}\frac{k_f}{k_i}\left(\sigma_{coh}S_{coh}(q,\omega) + \sigma_{inc}S_{inc}(q,\omega)\right) \quad (1)$$

Here are k_i and k_f are the incident and final wave vectors of the neutron beam where the scattering vector q is defined by $q = k_f - k_i$. The angular frequency ω is related to the measured energy transfer by $\omega = \Delta E/\hbar$ and Ω is the solid angle of detection. $S_i(q,\omega)$ are the coherent (i=coh) and incoherent (i=inc) dynamic structure factors (scattering functions) which are weighted by the corresponding scattering cross-sections for coherent and incoherent scattering σ_{coh} and σ_{inc}, respectively. PTCNSi1 and PTCNSi2g consist of hydrogen (H), carbon (C), and silicon (Si) (see Figure 1). This results for σ_{coh} and σ_{inc} in 103.9 barn and 1605.2 barn, respectively, for PTCNSi1 as well as 136.8 barn and 2247.3 barn for PTCNSi2g.[20] So for both polymers the measured scattering is predominantly incoherent.

For the neutron scattering experiments different spectrometers were combined.

Elastic scans: To gain an overview about the molecular dynamics at a time scale of ca. 2 ns fixed elastic window scans ($\Delta E \approx 0$) were carried out at a neutron backscattering spectrometer. The high-resolution spectrometer SPHERES[23,24] was utilized for that purpose. SPHERES is operated by the Jülich Centre for Neutron Science (JCNS) at the Heinz Maier-Leibnitz Zentrum (MLZ) in Garching, Germany. It is a cold neutron backscattering spectrometer of the third generation and is equipped with a focusing optics as well as a rotating phase-space-transform chopper and a linear doppler drive. Standard configuration was employed with an incident wavelength of $\lambda_n = 6.27$ Å leading to a maximal accessible elastic scattering vector of q=1.76 Å^{-1}. From the elastically scattered intensities an effective mean-square displacement $\langle u^2 \rangle_{eff}$ is calculated by a fractal model[25] which in case of a clear separation of elastic and inelastic scattering reduces to the usual Gaussian form

$$I_{el}(q)/I_0(q) = e^{(-q^2\langle u^2\rangle_{eff}/3)}. \quad (2)$$

Beside the separation of elastic/inelastic scattering the fractal model is also more reliable in a temperature range where the $\langle u^2 \rangle_{eff}$ values become large due to molecular motions, compared to the standard Gaussian approximation. In equ. 2, $I_{el}(q)$ and $I_0(q)$ are the elastically and totally scattered intensities where $I_0(q)$ was measured with increased statistics at 4 K. The experiments were carried out with a heating rate of 0.6 K/min for PTCNSi1 and 0.7 K/min for PTCNSi2g. This rate corresponds to 0.78 K and 0.97 K per data point.

Quasielastic measurements: To cover a broad time range for the quasielastic measurements neutron time-of-flight (TOF) spectroscopy was combined with neutron backscattering (BS).

The multi-chopper cold neutron time-of-flight spectrometer NEAT-2[26,27] was utilized for the TOF measurements. It was operated by the Helmholz-Zentrum Berlin (HZB). A configuration was employed with an incident wavelength of λ_n= 6 Å. The energy resolution was 64 µeV – 68 µeV (full width at half maximum) depending slightly on q with a maximal elastic scattering vector of q=2 Å^{-1}. Figure 2a depicts the incoherent dynamic structure factor for PTCNSi1 measured at NEAT-2 for different temperatures. For higher temperature the measured spectra show the characteristic quasielastic broadening in comparison to the resolution of the spectrometer R(q,ΔE) obtained by measurements of the sample at 3.5 K. For the latter it was assumed that all molecular fluctuations leading to quasielastic scattering are frozen besides quantum zero-point motions.

For the neutron backscattering measurements IN16B was employed operated by the Institut Laue-Langevin (ILL) in Grenoble, France.[28] IN16B is a cold neutron backscattering spectrometer of the third generation with a focusing optic, a rotating phase-space-transform chopper and a linear doppler drive. It was employed in the standard high flux configuration with unpolished Si-111 monochromators/analyzers and an incident wavelength of λ_n= 6.27 Å. This configuration results in a resolution of 0.74…0.81 µeV. The maximal accessible elastic scattering vector was q=1.83 Å^{-1}. Examples for S_{Inc}(q, ΔE) for PTCNSi1 measured at IN16B are shown in Figure 2b. Like the TOF data also the backscattering spectra show the quasielastic broadening compared to the resolution of the spectrometer measured at 2 K.

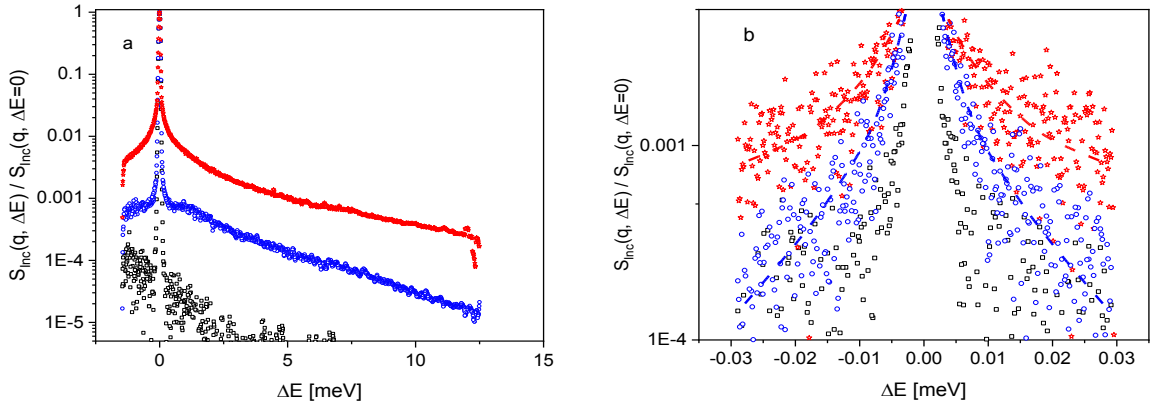

Figure 2: a) Incoherent dynamical structure factor S_{Inc}(q,ΔE) normalized by the height of the elastic line measured for PTCNSi1 at NEAT-2 at an q vector of 1.61 Å^{-1}: black squares – resolution (3.5 K); blue - circles – 75 K, red asterisks – 275 K. b) Incoherent dynamical structure factor S_{Inc}(q,ΔE) normalized by the height of the elastic line measured for PTCNSi1 at IN16B at an angle of 88 °: black squares – resolution (2 K); blue - circles – 75 K, red asterisks – 275 K. Lines are guides for the eyes.

The program Mantid[29] was used to evaluate the NEAT-2 data which features TOF to energy conversion, background subtraction, Vanadium normalization, and self-attenuation correction. Mantid was also used for the data reduction of the backscattering data where Vanadium normalization were applied together with self-attenuation correction as well as an attenuation correction on the background to be subtracted. For both data sets an effective but cross section weighted $S_{Inc}(q,\Delta E)$ was obtained.

Figure 2 evidences the large difference in the energy resolution of the time-of-flight and the backscattering data. To analyze the results from NEAT-2 and IN16B jointly both sets of data were Fourier transformed and divided by the corresponding Fourier transform of the resolution. By that procedure absolute values of the incoherent intermediate scattering function $S_{Inc}(q,t)$ were obtained. Furthermore, both the NEAT-2 and the IN16B data were corrected for multiple scattering. Because the exact scattering geometry is not known for that correction, in the time domain a multiple scattering fraction was fitted to optimize the limit $S_{inc}(q\rightarrow 0,t)=1$.[30] The estimated multiple scattering fractions with respect to single scattering for PTCNSi1 were 16% and 20% for IN16B and NEAT respectively and for PTCNSi2g 24% and 25%.

3. Results and Discussion

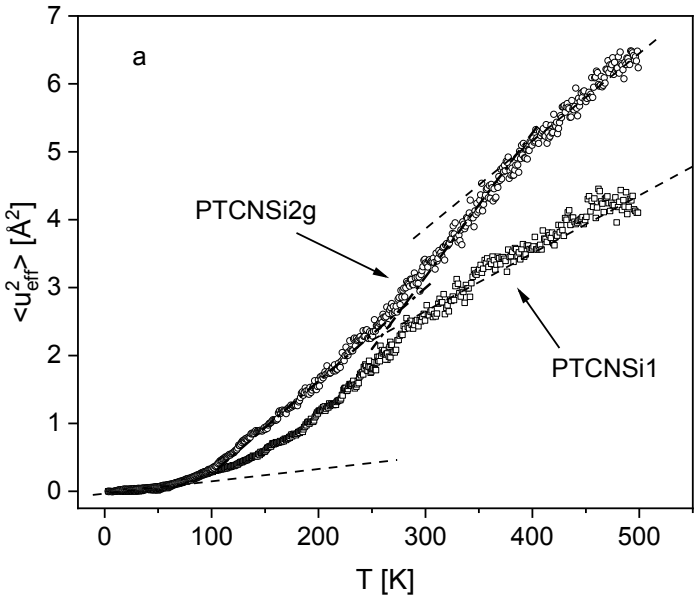

Figure 3a: Effective mean squared displacement $\langle u^2_{eff} \rangle$ versus temperature: squares – PTCNSi1, circles – PTCNSi2g. Lines are guides for the eyes.

The temperature dependence of the effective mean squared displacement for PTCNSi1 and PTCNSi2g is depicted in Figure 3a. For both materials the temperature dependence of $\langle u^2_{eff} \rangle(T)$ at low temperatures is due to vibrations. In the temperature range from 150 K to 275 K for PTCNSi1 the temperature dependence of the effective mean squared displacement shows a step-like change. This step indicates the onset of molecular motions at a time scale of ca. 2 ns. By means of dielectric spectroscopy, sensitive to molecular fluctuations connected to a dipole moment, no relaxation process was detected for PTCNSi1 in this temperature range.[14] Therefore, it has to be concluded that the observed relaxation process is related to nonpolar groups. The only molecular moieties which can be mobile at these low temperatures and which are not polar, i.e. do not contain any polar bonds or dipole moments, are the methyl groups. It is also known from the literature that the methyl group for conventional polymers becomes active in that temperature range.[30-33] Therefore, the step observed in $\langle u^2_{eff} \rangle(T)$ for PTCNSi1 is assigned to the methyl group rotation.

For PTCNSi2g a different behavior is observed in the temperature dependence of the effective mean squared displacement. Firstly, at temperatures higher than 100 K $\langle u^2_{eff} \rangle(T)$ for PTCNSi2g is higher than that for PTCNSi1. Secondly, after a first increase of the mean squared displacement which occurs almost in parallel to that of PTCNSi1 there seems to be a further change in the temperature dependence of $\langle u^2_{eff} \rangle(T)$ for PTCNSi2g. This might indicate a second process in addition to that what is observed for PTCNSi1. This possible second process could be also assigned to a methyl group rotation, but with a higher activation barrier. It should be noted that also dielectric spectroscopy reveals two different β-relaxation processes for PTCNSi2g at higher temperatures which is not the case for PTCNSi1.[14] Also a bimodal size distribution of the microporosity was reported for PTCNSi2g.[7,8] As concluded also in ref. [14] the morphology of PTCNSi2g is more heterogeneous than that of PTCNSi1.

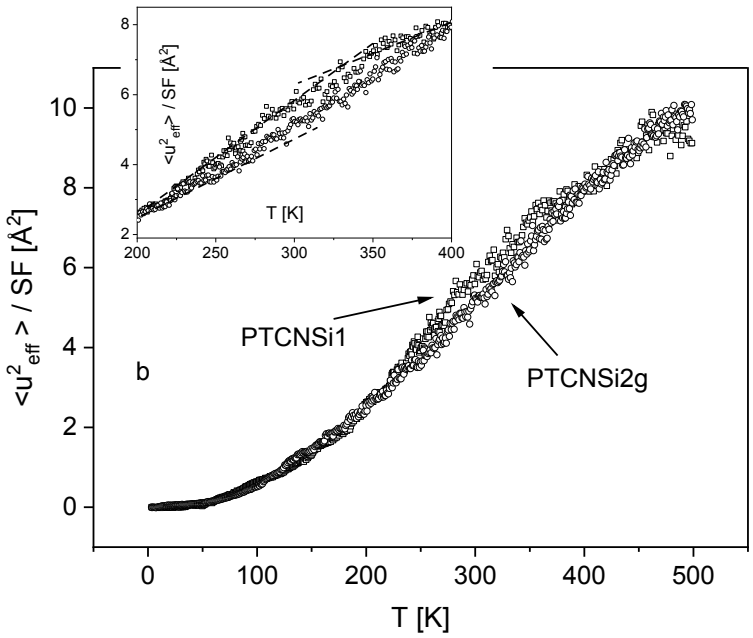

Figure 3b: Effective mean squared displacement $\langle u^2_{eff} \rangle$ versus temperature normalized by the scaling factor SF described in the text: squares – PTCNSi1, circles – PTCNSi2g. The inset enlarges the data in the temperature range from 200 K and 400 K. Lines are guides for the eyes.

To understand the difference in the temperature dependence of $\langle u^2_{eff} \rangle$(T) for both materials one has to consider that PTCNSi1 has three methyl groups while PTCNSi2g has six (see Figure 1). A scaling by the factor SF= (3 * number of methyl groups) / (number of all protons in the repeating unit) should lead to a collapse of $\langle u^2_{eff} \rangle$(T) for both polymers when the number of methyl groups per repeat unit is the only difference in the behavior between PTCNSi1 and PTCNSi2g. Figure 3b reveals that the reduced values of the effective mean squared displacement overlap up to ca. 250 K. In the temperature range from ca. 250 K to 375 K differences between both data sets are observed where the normalized values for PTCNSi2g are lower than those obtained for PTCNSi1. The inset of Figure 3b reveals that the differences in both data sets are significant considering the uncertainty of the measurement reflected by the scatter of the data. This result means that compared to PTCNSi1 for PTCNSi2g the rotation of some the methyl groups are not thermally activated in that temperature range. The distinct deviations in the normalized mean squared displacement data indicate a significant difference of the motional processes connected to the methyl group rotation of the two polymers. For

temperatures above 375 K the data measured for PTCNSi1 and PTCNSi2g show again the same temperature dependence.

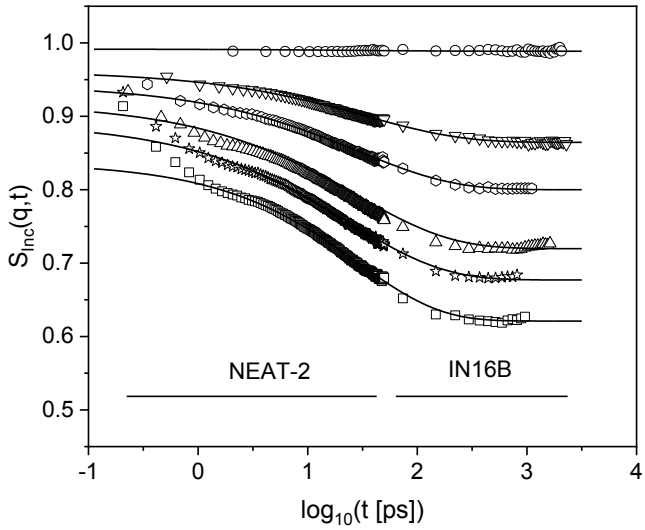

Figure 4. Incoherent intermediated scattering function $S_{Inc}(q,t)$ versus time for PTCNSi1 for different q vectors at 150 K: circles – 0.3 Å^{-1}, down sided triangles – 0.84 Å^{-1}, octagons – 1.13 Å^{-1}, triangles – 1.4 Å^{-1}, asterisk – 1.61 Å^{-1} and squares – 1.78 Å^{-1}. Lines are fits of equ. 3 to the corresponding data.

To investigate the molecular dynamics further quasielastic neutron scattering is employed. Figure 4 depicts the time dependent intermediate scattering function $S_{Inc}(q,t)$ at 150 K for different q-vectors for PTCNSi1. In the time range 0.1 ps to ca. 50 ps the data correspond to the neutron time of flight measurements at NEAT-2, whereas the data for longer times than 50 ps were measured by neutron backscattering at IN16B. Figure 4 proves that the measurements results obtained from both spectrometers do nicely match. A single decay was observed for $S_{Inc}(q,t)$ indicating a relaxation process. As discussed above this relaxation process is assigned to the methyl group rotation in PTCNSi1. The Rotation Rate Distribution Model (RRDM)[31] is the standard model for the methyl group rotation. Here a simplified treatment is used: a stretched exponential function

$$S_{Inc}(q,t) = DWF * \left((1 - EISF_M) \exp\left(-\left(\frac{t}{\tau_M} \right)^{\beta_M} \right) + EISF_M \right) \quad (3)$$

is fitted to the data. DWF is the Debye-Waller factor, β_M is the stretching parameter describing the distribution of relaxation times and τ_M is the relaxation time for methyl group rotation. The Elastic Incoherent Structure Factor is denoted by $EISF_M$. Figure 4 shows also that the data can be well described by equ. 3. Values of β_M are given in the SI, Table S1.

The q-dependence of the $EISM_M$ for PTCNSi1 is depicted in Figure 5a. The most straightforward model to calculate the Elastic Incoherent Structure Factor for methyl group rotation is a jump diffusion in a three-fold potential $V(\phi) \sim (1 - \cos(3\phi))/2$.[31,34] It considers three equivalent energy minima with respect to the rotation angle ϕ of the methyl group. This model gives for the $EISF_M$

$$EISF_M(q) = \frac{1}{3}\left(1 + 2\frac{\sin(\sqrt{3}\,qr)}{\sqrt{3}\,qr}\right). \quad (4)$$

Here r= 1.027 Å describes the radius of a circle spanned by the positions of the hydrogen nuclei of the methyl group. Figure 5a shows that the data obtained for PTCNSi1 do not follow equ. 4. To understand this discrepancy, one must consider that not all hydrogen nuclei are involved in the methyl group rotation. For PTCNSi1, the monomeric unit has 20 hydrogen nuclei of which only 9 are situated in methyl groups. Therefore, 11 hydrogens do not participate in the methyl group rotation and scatter elastically in the temperature range relevant for the methyl group rotation. The corresponding fraction of hydrogens which scatter elastically C_{fix} is (20-9)/20=0.55 which must be considered in equ. 4 as[30,32,33]

$$EISF_{M,corr}(q) = (1 - C_{fix})EISF_M(q) + C_{fix}. \quad (5)$$

Figure 5a shows that equ. 5 describes the data reasonably well with the $EISF_M$ from equ. 5 taking into account the theoretical fraction C_{fix}=0.55. A best fit of equ. 5 to the data yields an effective C_{fix}=0.52 which is quite close to the theoretical value. This provides further evidence that the observed relaxation process is indeed the methyl group rotation. The slight difference

between the theoretical C_{fix} and the fitted value might be due to experimental error or that a small amount of methyl groups is hindered in its rotation.

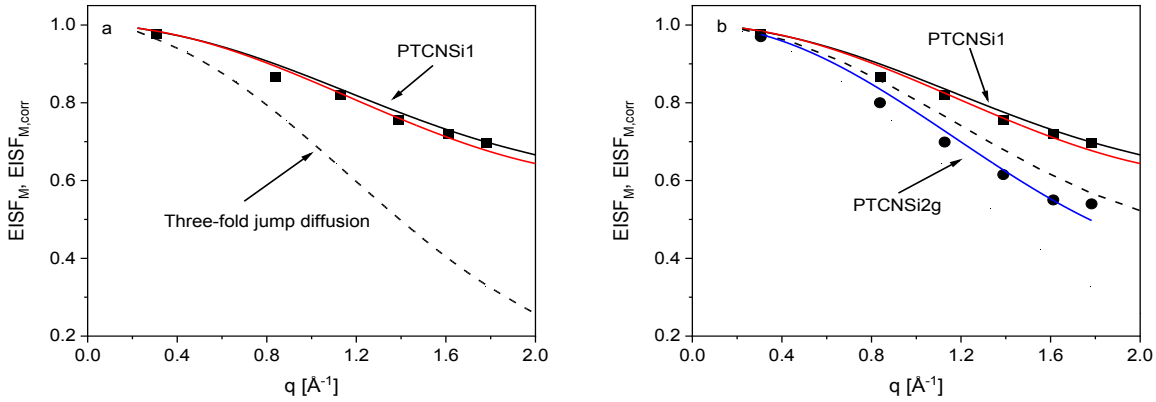

Figure 5: a) Squares - q dependence of the elastic incoherent structure factor $EISF_M$ for PTCNSi1 at T=200 K. Dashed line - calculated dependence according to equ. 4. Black line – calculated according to equ. 5 with the theoretical fraction C_{fix}=0.55. Red line – Fitting of equ. 5 to the data which results in C_{fix}=0.52.
b) Comparison of the q dependence of the $EISF_M$ for PTCNSi1 (squares) and PTCNSi2g (circles) at 200 K. Black line – calculated according to equ. 5 for PTCNSi1 with the theoretical fraction C_{fix}=0.55. Red line – Fitting of equ. 5 to the data of PTCNSi1 which results in C_{fix}=0.52. Dashed black line – calculated according to equ. 5 for PTCNSi2g with the theoretical fraction C_{fix}=0.357. Blue line – Fitting of equ. 5 to the data of PTCNSi2g which results in C_{fix}=0.253.

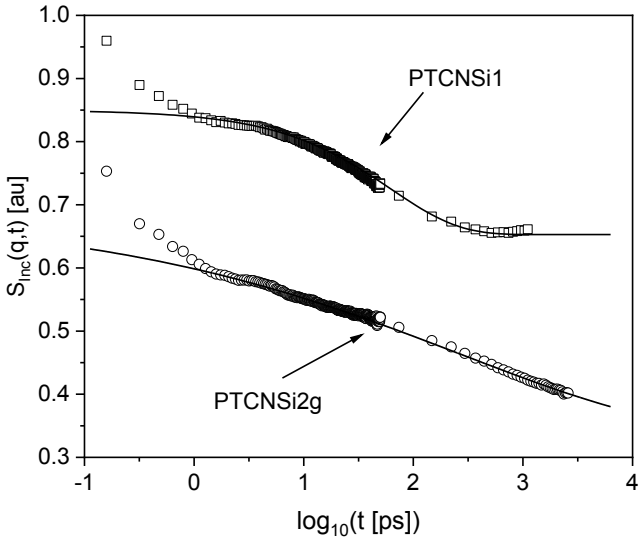

Figure 6. Comparison of the incoherent intermediate scattering function $S_{Inc}(q,t)$ versus time for PTCNSi1 (squares) and PTCNSi2g (circles) at q=1.78 $Å^{-1}$ and T=125 K. Lines are fits of equ. 3 to the corresponding data. The data are shifted along the y-scale for sake of clarity.

Figure 6 compares the time dependent intermediate scattering function for PTCNSi1 and PTCNSi2g at the same temperature of T=125 K and q=1.78 $Å^{-1}$. Compared to PTCNSi1, the $S_{Inc}(q,t)$ measured for PTCNSi2g is stretched of a much broader time range. On the one hand, this might be due to two relaxation processes involved in $S_{Inc}(q,t)$. This interpretation would be in agreement with the temperature dependence of the mean squared displacement (see Figure 3). Nevertheless, no clear two-step decay could be observed in the time dependent intermediate scattering function of PTCNSi2g. Moreover, two stretched exponential functions could not be fitted unambiguously to the data. On the other hand, the "stretching" of $S_{Inc}(q,t)$ for PTCNSi2g might also be due to a broad distribution of activation energy barriers for the methyl group rotation related to the their sterically slightly hindered arrangement. For both reasons, equ 3 is also used to analyze the data of PTCNSi2g. Values of β_M are given in the SI, Table S1.

Figure 5b compares the q dependence of the EISF for PTCNSi1 and PTCNSi2g. PTCNSi2g contains 28 hydrogen nuclei in the repeat unit of which 18 hydrogen nuclei are in methyl groups. This yields 0.357 as the theoretical value of C_{fix}. Figure 5b shows that in contrast to PTCNSi1, equ. 5 with the theoretical value of C_{fix} does not describe the data of PTCNSi2g. Rather, a fit of equ. 5 to the data of PTCNSi2g leads to 0.253 for C_{fix} which is considerably lower than the theoretical value calculated from the chemical structure. This difference cannot be explained as result from experimental errors. Therefore, it must be concluded that for PTCNSi2g a considerable number of methyl groups is hindered in their rotation. It can be seen from Figure 1 that the arrangement of the methyl groups in PTCNSi2g is sterically demanding.

For a free rotation enough free space must be available in the vicinity of the respective methyl group. Whether this space is available or not might depend also on the rotational positions of adjacent methyl groups attached to the second Si atom in the same repeating unit as well as their hydrogen nuclei. This discussion assumes that a rotation of the Si group around the single bond to the butene cycle is frozen at these temperatures.

The analysis of time dependence of $S_{Inc}(q,t)$ gives also the relaxation time τ_M of the methyl groups. For a local 3-fold jump diffusion process the relaxation time should be independent of the scattering vector q. This is indeed observed for PTCNSi1 and PTCNSi2g. The relaxation rates for the methyl group rotation are depicted for PTCNSi1 and PTCNSi2g in Figure 7 where τ_M is plotted versus inverse temperature in Arrhenius coordinates. The data for both polymers can be described by the Arrhenius equation which reads

$$\tau_M = \tau_\infty \exp\left(\frac{E_A}{RT}\right) \quad (6)$$

where E_A is the activation energy, τ_∞ is the relaxation time at infinite temperatures, and R is the universal gas constant. For PTCNSi1 an activation energy of 4.2 kJ/mol with a prefactor of $\log_{10}(\tau_\infty\ [s])$= -12.1 is obtained which is comparable to data obtained for the methyl group rotation of poly(methyl phenyl siloxane) (PMPS).[32] PMPS is a quite flexible polymer for which it can be expected that the methyl groups can rotate freely. From the similar value of the activation energy of the methyl group of PMPS and PTCNSi1 it can be concluded that methyl groups can also rotate freely in PTCNSi1. This is further confirmed by the value of $\log_{10}(\tau_\infty\ [s])$= -12.1 which is in the typical range expected for a thoroughly localized process. This conclusion is also in agreement with the q-dependence of the elastic incoherent structure factor.

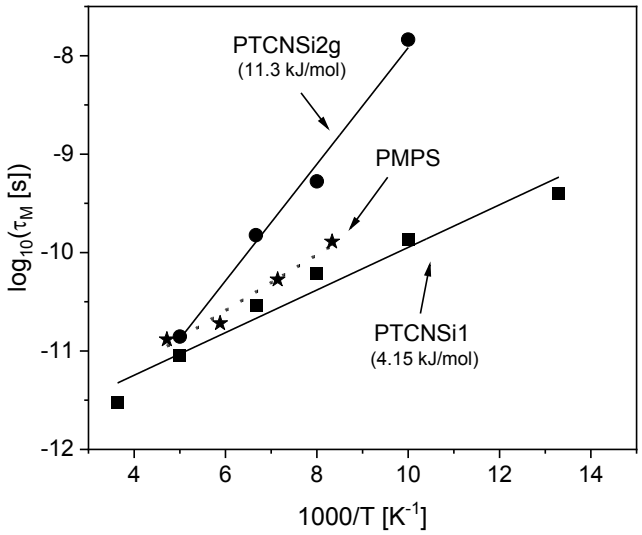

Figure 7. Relaxation time for the methyl group rotation versus inverse temperature: Squares – PTCNSi1, circles – PTCNSi2g and asterisk – poly(methyl phenyl siloxane) (PMPS). The data for PMPS was taken from ref. 32. Lines are fits of the Arrhenius equation to the corresponding data.

For PTCNSi2g it was found that the activation energy (11.3 kJ/mol) is almost three times higher than the value estimated for PTCNSi1 (4.2 kJ/mol). This result is in direct agreement with the conclusion drawn from the q-dependence of the EISF, i.e., that the methyl group rotation is sterically hindered for PTCNSi2g in comparison to PTCNSi1. Moreover, for the prefactor $\log_{10}(\tau_\infty$ [s]) a value of -13.8 is obtained which is not typical for a localized molecular process. This means that besides enthalpic also entropic contributions are involved in the relaxation process. On the one hand, these entropic contributions can be assigned to the steric hinderance of the methyl group rotation. On the other hand, the smaller value of the prefactor can be also discussed in terms of the so-called compensation rule (Meyer/Neldel rule).[35-38]it seems to be clear that the physical reason for the compensation law is directly related to the cooperativity of the underlying process. Regarding the methyl group rotation, it can be assumed that due to

the sterically arrangement of the CH_3-groups in PTCNSi2g, they can only rotate when they move – at least in part - somehow cooperatively together.

4. Conclusion

A combination of neutron time-of-flight and neutron backscattering is employed to carry out quasielastic neutron scattering experiments to investigate the molecular dynamics of two addition-type poly(tricyclononenes) with Si-substituted bulky side groups, PTCNSi1 and PTCNSi2g on a broad time scale from 0.1 ps to 3 ns. While PTCNSi1 bears three methyl groups in the monomeric unit (-$Si(Me)_3$), PTCNSi2g has six (two -$Si(Me)_3$). Therefore, the arrangement of the methyl groups is sterically more demanding for PTCNSi2g compared to PTCNSi1. The Si-substituted bulky side groups give rise to a considerable microporosity characterized by high BET surface area values of 790 m^2/g (PTCNSi2g)[7] and 610 m^2/g (PTCNSi1). The microporosity results in a rather high gas permeability for both polymers. In combination with reasonable permselectivities these two polymers are considered as promising materials as separation layer in gas separation membranes. Molecular motions like methyl group rotations might change the structure of the temporarily interconnected microporous network by opening and closing channels or bottlenecks between voids providing pathways for gas transport processes. This might be the molecular reason for the good permselectivity of these polymers. It should be also noted that the molecular mobility of the methyl groups might be also related to the physical aging of these systems as discussed for the archetype of polymers of intrinsic microporosity PIM-1 by NMR measurements.[39]

To obtain an overview about the molecular dynamics, elastic scans were carried out on a neutron backscattering spectrometer. For both polymers the effective mean squared displacement reveals one relaxation process which is assigned to the methyl group rotation.

To analyze the time-of-flight and the backscattering data jointly together, the dynamic structure factors are Fourier transformed and divided by the Fourier transform of the corresponding

resolution measured at low temperatures. Absolute values of the incoherent intermediate scattering function $S_{Inc}(q,t)$ were obtained by this procedure. A single step-like decay was observed in $S_{Inc}(q,t)$ for which a stretched exponential was used to further analyze the data. This analysis results in the EISF in its q-dependence and relaxation time. The diffusional jump rotation in a threefold potential, the standard model for the methyl group rotation, was employed to analyze the q-dependence of the EISF. For PTCNSi1 it was found that more or less all methyl groups participate in the methyl group rotation. This is different for PTCNSi2g where a considerable amount of methyl groups is blocked or hindered in their rotation. This result is discussed by the sterically complex arrangement of the methyl groups in PTCNSi2g compared to PTCNSi1. This line of argumentation is further supported by the result that the estimated value of the activation energy for the methyl group rotation of PTCNSi2g is approximately three times higher than the value found for PTCNSi1.

Corresponding Author

A. Schönhals, Bundesanstalt für Materialforschung und -prüfung (BAM), Unter den Eichen 87, 12205 Berlin, Germany; Email: Andreas.Schoenhals@bam.de

Author's contributions

AS initiated the work, MK prepared the sample films for neutron scattering; RZ, PS, GG, MR, MA, BF and AS carried out the measurements; all the data analysis were carried out by RZ, GG, MR, MA and AS; DA and MB synthesized the polymers, MBoe significantly contributed to the discussion and finalization of the manuscript. The manuscript was written by

contributions of all authors. All authors have given approval to the final version of the manuscript.

Notes

The authors declare no competing financial interest.

Acknowledgements

The Helmholz Zentrum Berlin (HZB, Berlin, Germany), the Heinz Maier-Leibnitz Zentrum Garching (MLZ, Garching, Germany), and the Institut Laue-Langevin (ILL, Grenoble, France) are thanked for enabling the neutron scattering experiments. The synthesis of Si-containing addition polynorbornenes was carried out within the State Program of TIPS RAS.

References:

1 Higashimura, T.; Masuda, T.; Okada, M. Gas Permeability of Polyacetylenes with Bulky Substituents. *Polym. Bull.* **1983,** *10* (1), 114-117.

2 Masuda, T.; Kawasaki, M.; Okano, Y.; Higashimura, T. Polymerization of Methylpentynes by Transition Metal Catalysts: Monomer Structure, Reactivity, and Polymer Properties. *Polym. J.* **1982,** *14* (5), 371-377.

3 Morisato, A.; Pinnau, I. Synthesis and Gas Permeation Properties of Poly(4-methyl-2-pentyne). *J. Membr. Sci.* **1996,** *121* (2), 243-250.

4 Budd, P. M.; Msayib, K. J.; Tattershall, C. E.; Ghanem, B. S.; Reynolds, K. J.; McKeown, N. B.; Fritsch, D. Gas Separation Membranes from Polymers of Intrinsic Microporosity. *J. Membr. Sci.* **2005,** *251* (1–2), 263-269.

5 Carta, M.; Malpass-Evans, R.; Croad, M.; Rogan, Y.; Jansen, J. C.; Bernardo, P.; Bazzarelli, F.; McKeown, N. B. An Efficient Polymer Molecular Sieve for Membrane Gas Separations. *Science* **2013,** *339* (6117), 303-307.

6 Yampolskii, Y. P. A Current Position of Polyacetylenes Among Other Highly Permeable Membrane Materials. *Polym. Rev.* **2017,** *57* (1), 200-212.

7 Chapala, P. P.; Bermeshev, M. V.; Starannikova, L. E.; Belov, N. A.; Ryzhikh, V. E.; Shantarovich, V. P.; Lakhin, V. G.; Gavrilova, N. N.; Yampolskii, Y. P.; Finkelshtein, E. S. A Novel, Highly Gas-Permeable Polymer Representing a New Class of Silicon-Containing Polynorbornens as Efficient Membrane Materials. *Macromolecules* **2015,** *48* (22), 8055-8061.

8 Gringolts, M.; Bermeshev, M.; Yampolskii, Y.; Starannikova, L.; Shantarovich, V.; Finkelshtein, E. New High Permeable Addition Poly(tricyclononenes) with $Si(CH_3)_3$ Side Groups. Synthesis, Gas Permeation Parameters, and Free Volume. *Macromolecules* **2010,** *43*, 7165-7172.

9 Alentiev, D. A.; Bermeshev, M. Design and synthesis of porous organic polymeric materials from norbornene derivatives. *Polym. Rev.* **2021**, 38, DOI: 10.1080/15583724.2021.1933026

10 Wang, X.; Wilson, T. J.; Alentiev, D.; Gringolts, M.; Finkelshtein, E.; Bermeshev, M.; Long, B. K. Substituted polynorbornene membranes: a modular template for targeted gas separations. *Polym. Chem.* **2021**, 12, 2947-2977.

11 Hofmann, D.; Heuchel, M.; Yampolskii, Y.; Khotimskii, V.; Shantarovich, V. Free Volume Distributions in Ultrahigh and Lower Free Volume Polymers: Comparison between Molecular Modeling and Positron Lifetime Studies. *Macromolecules* **2002,** *35* (6), 2129-2140.

12 Heuchel, M.; Fritsch, D.; Budd, P. M.; McKeown, N. B.; Hofmann, D. Atomistic Packing Model and Free Volume Distribution of a Polymer with Intrinsic Microporosity (PIM-1). *J. Membr. Sci.* **2008,** *318* (1-2), 84-99.

13 Yin, H.; Chapala, P.; Bermeshev, M.; Schönhals, A.; Böhning, M. Molecular Mobility and Physical Aging of a Highly Permeable Glassy Polynorbornene as Revealed by Dielectric Spectroscopy. *ACS Macro Lett.* **2017**, 6, 813-818.

14 Yin, H.; Chapala, P.; Bermeshev, M.; Pauw, B. R.; Schönhals, A.; Böhning. M. Influence of trimethylsilyl side groups on the molecular mobility and charge transport in highly permeable glassy polynorbornenes ACS Applied Polymer Materials **2019**, 1, 844-855

15 Mazo, M.; Balabaev, M.; Alentiev, A.; Yampolskii, Y. Molecular Dynamics Simulation of Nanostructure of High Free Volume Polymers with $SiMe_3$ Side Groups *Macomolecules* 2018, 51, 1398 – 1408.

16 Inoue, R.; Kanaya, T.; Masuda, T.; Nishida, K.; Yamamuro, O. Relationship between the Local Dynamics and Gas Permeability of Para-Substituted Poly(1-chloro-2-phenylacetylenes) *Macromolecules* **2012**, 45, 6008-6014.

17 Kanaya, T.; Teraguchi, M.; Masuda, T.; Kaji, K. Local mobility of substituted polyacetylenes measured by quasielastic neutron scattering and its relationship with gas permeability *Polymer* **1999**, 40, 7157−7161.

18 Kanaya, T.; Tsukushi, I.; Kaji, K.; Sakaguchi, T.; Kwak, G.; Masuda, T Role of Local Dynamics in the Gas Permeability of Glassy Substituted Polyacetylenes. A Quasielastic Neutron Scattering Study *Macromolecules* **2002**, 35, 5559−5564.
19 Zorn, R.; Lohstroh, W.; Zamponi, M.; Harrison, W. J.; Budd, P. M.; Böhning, M.; Schönhals, A. Molecular mobility of a polymer of intrinsic microporosity revealed by quasielastic neutron scattering. *Macromolecules* **2020**, 53, 6731-6739.
20 Zorn, R.; Szymoniak, P.; Kolmangadi, M. A.; Wolf, M.; Alentiev, D, A; Bermeshev, M.; Böhning, M.; Schönhals, A. Low frequency vibrational density of state of highly permeable super glassy polynorbornenes – the Boson peak *Phys. Chem. Chem. Phys.* **2020**, 22, 18381-18387.
21 Alentiev, D. A.; Bermeshev, M.; Starannikova, L. E.; Bermesheva, E. V.; Shantarovich, V. P.; Bekeshev, V. G.; Yampolskii, Y. P.; Finkelshtein, E. S. Stereoselective synthesis and polymerization of exo-5-trimethylsilylnorbornens *J. Polym. Sci, Polym. A Chem.* **2018**, 56, 1234-1248.
22 Bée, M. Quasielastic neutron scattering. Principles and applications in solid state chemistry, biology and materials science, Adam Hilger, Bristol, UK **1988**.
23 Heinz Maier-Leibnitz Zentrum, SPHERES: Backscattering spectrometer *Journal of large-scale research facilities* **2015**, 1, A30. http://dx.doi.org/10.17815/jlsrf-1-38
24 Wuttke, J.; Budwig, A.; Drochner, M.; Kämmerling, H.; Kayser, F.-J.; Kleines, H.; Ossovyl, V.; Pardo, L- C.; Prager, M.; Richter, D.; Schneider, G. J.; Schneider, H.; Staringer, S. SPHERES, Jülich's high-flux neutron backscattering spectrometer at FRM II *Rev. Sci. Instr.* 2012, 83, 075109.
25 Zorn, R. Nucl. Instr. Meth. A 2009, 603, 439-445.
26 Russina, M.; Guenther, G.; Grzimek, V.; Gainov, R.; Schlgel, M.-C.; Drescher, L.; Kaulich, T.; Graf, W.; Urban, B.; Daske, A.; Grotjahn, K.; Hellhammer, R.; Buchert, G.; Kutz, H.; Rossa, L.; Sauer, O.-P.; Fromme, M.; Wallacher, D.; Kiefer, K.; Klemke, B.; Grimm, N.; Gerischer, S.; Tsapatsaris, N.; Rolfs, K. Upgrade Project NEAT′2016 at Helmholtz Zentrum Berlin – What can be done on the medium power neutron source Physica B Condensed Matter, 551 (2018), 506-511.
27 Guenther, G.; Russina, M. Background optimization for the neutron time-of-flight spectrometer NEAT Nuclear Instruments and Methods in Physics. Research A 828 (2016) 250–261.
28 Schönhals, A.; Appel, M.; Frick, B.; Szymoniak, P.; Zorn, R. Quasielastic Neutron Backscattering Measurements on Highly Permeable Glassy Polynorbornenes. Institut Laue-Langevin (ILL) **2020**, doi:10.5291/ILL-DATA.6-04-278
29 Arnold, O. et al. Mantid—Data analysis and visualization package for neutron scattering and μSR experiments, Nuclear Instruments and Methods in Physics Research Section A, 764, 2014, 156-166
30 Zorn, R.; Frick, B.; Fetters, L. Quasielastic neutron scattering study of the methyl group dynamics in polyisoprene *Journal of Chemical Physics* **2002**, 116, 845-853.
31 Colmenero, J.; Moreno, A.; Alegria, A. Neutron scattering investigations on methyl group dynamics in polymers *Progress in Polymer Science* **2005**, 30, 1147-1184.
32 Schönhals, A. Schick, C.; Huth, H.; Frick, B.; Mayorova, M.; Zorn, R. Molecular Dynamics in Glass-forming Poly(phenyl methyl siloxane) as Investigated by Broadband Thermal, Dielectric and Neutron Spectroscopy *J. Non-Cryst. Solids* **2007**, **353**, 3853-3861.
33 Schönhals, A.; Zorn, R.; Frick, B. Inelastic Neutron Spectroscopy as a Tool to Investigate Nanoconfined Polymer Systems *Polymer* **105** (2016) 393-406
34 Prager, M.; Heidemann, A. Rotational Tunneling and Neutron Spectroscopy: A Compilation *Chem. Rev.* **1997**, 97, 2933-2966.
35 Dyre, J. C. A phenomenological model for the Meyer-Neldel rule. *J. Phys. C: Solid State Phys.* **1986**, 19, 5655-5664.

36 Yelon, A.; Movaghar, B.; Branz, H. M. Origin and consequences of the compensation (Meyer-Neldel) law. *Phys. Rev. B* **1992**, 46, 12244
37 Schönhals, A.; Wolff, D., Springer, J. Influence of the mesophase structure on the β-relaxation in comb-like polymetharylates. *Macromolecules* **1995**, 28, 6254-6257.
38 Schönhals, A.; Wolff, D., Springer, J. Influence of the mesopphase structure on the β-relaxation in liquid crystalline poly (meth) acrylates. *Polymer Advanced Technologies* **1996**, 7, 853
39 Lau, C. H.; Nguyen, P. T. Hill, M. R.; Thornton, A. W.; Konstas, K.; Doherty, C. M; Mulder, R. J.; Bourgeois, L.; Liu, A. C. J.; Sprouster, D. J.; Sullivan, J. P; Bastow, T. J.; Hill, A. J.; Gin, D. L; Noble, R. D. Ending Aging in Super Glassy Polymer Membranes *Angew. Chem. Int. Ed.* **2014**, 53, 5322 –5326